World Cancer Research Journal
WCRJ 2026; 13: e3040
DOI: 10.32113/wcrj_202605_3040

PHAGE-ASSISTED CRYPTOTANSHINONE DELIVERY SUPPRESSES *FOXM1* AND REDUCES THE VIABILITY OF MCF-7 BREAST CANCER CELLS

B. USTUNDAG[1], M. USTUNDAG[2]

[1]Department of Scientific Research Project Office, Van Yuzuncu Yil University, Van, Türkiye
[2]Department of Chemistry and Chemical Management Technologies, Muradiye Vocational School, Van Yuzuncu Yil University, Van, Türkiye

Corresponding Author
Mustafa Ustundag, MD; e-mail: mustafaustundag@yyyu.edu.tr; m.ustundg@gmail.com

ABSTRACT – *Objective:* This study aimed to evaluate the anticancer activity of cryptotanshinone (CPT) in estrogen and progesterone receptor-positive (ER+/PR+) MCF-7 breast cancer cells and to determine whether delivery via the filamentous M13 bacteriophage enhances CPT's functional effect, with a focus on *FOXM1* gene expression.

Materials and Methods: MCF-7 cells were treated with CPT across a concentration range to establish dose-response behavior and calculate IC_{50} values at 24 and 48 h using an MTT viability assay. For phage-mediated delivery, cells were exposed to M13 alone, free CPT, CPT co-administered with M13 without loading, and preformed M13–CPT complexes, followed by MTT-based viability assessment. *FOXM1* messenger ribonucleic acid (mRNA) levels were quantified at 24 and 48 h by quantitative reverse transcription polymerase chain reaction (qRT-PCR) and normalized to a housekeeping gene using ΔCt-based analysis.

Results: CPT decreased cell viability in a dose- and time-dependent manner, yielding IC_{50} values of 19.82 µM at 24 h and 16.14 µM at 48 h. CPT also suppressed *FOXM1* expression, with a stronger inhibitory effect at 48 h rather than at 24 h. M13 alone did not produce a meaningful change in viability. Compared with free CPT and the non-loaded CPT+M13 mixture, M13–CPT induced a markedly greater reduction in cell viability. In addition, Annexin V-fluorescein isothiocyanate/propidium iodide (V-FITC/PI) analysis showed that CPT increased apoptosis, with a stronger effect in the M13–CPT group than free CPT.

Conclusions: CPT reduces MCF-7 cell viability and downregulates *FOXM1* expression, and delivery through M13 bacteriophage further enhances *in vitro* cytotoxic efficacy without requiring additional targeting ligands.

KEYWORDS: Bacteriophage, Breast cancer, Cryptotanshinone, M13.

INTRODUCTION

Breast cancer, with a steadily rising incidence and rapid spread, particularly among women, is one of the most dangerous forms of cancer. Based on current 2025 data (with more than 2.3 million new cases), it is defined as the most frequently diagnosed malignancy among women worldwide; moreover, breast cancer accounts for approximately 11.7% of overall cancer data[1]. Due to problems such as poor prognosis in advanced-stage and metastatic breast cancer cases and the inability to obtain the desired outcome from existing treatment methods, oncological research has focused on the development of new and specific treatment strategies[2]. Breast cancer is a complex disease in which the response to treatment is variable due to its molecular heterogeneity. This situation necessitates the development of new target-oriented and mechanism-based research. The MCF-7 cell line, which is characterized by estrogen and progesterone receptor positivity (ER+/PR+), is a frequently used *in vitro* standard in breast cancer research[3].

Cryptotanshinone (CPT), isolated from Salvia miltiorrhiza by biotechnological methods, stands out as a natural compound that exhibits antiproliferative effects and has been associated with apoptosis-related mechanisms in various cancer cell lines, and it has been proven to show anticancer potential through its suppressive effect on signal transducer and activator of transcription 3 (STAT3), phosphoinositide 3-kinase/protein kinase B (PI3K/AKT), and mitogen-activated protein kinase (MAPK) signaling pathways[4]. In various cancer studies[5], it has been reported that CPT arrests the cell cycle at the G2/M phase in breast cancer cells, suppresses cell proliferation, and induces apoptosis. In addition, CPT has been shown to have various effects, such as affecting the expression levels of various genes associated with the regulation of the cell cycle, mitotic control, and cellular survival[6].

The *FOXM1* gene, which plays a role in cell cycle and proliferation processes, is one of the genes that plays a critical role in the regulation of mitotic progression and the G2/M phase transition[7,8]. Changes in the expression levels of this gene are accepted as the gold standard in evaluating tumor aggressiveness and treatment response[7]. However, the transcriptional effect of CPT on this specific gene panel in the MCF-7 cell line has not yet been elucidated in detail. Studies in the literature in which the effects of CPT on *FOXM1* expression in MCF-7 cells are comparatively evaluated between its free form and phage-carried form are limited.

While CPT is expected to change the expression level of this gene and this change is expected to have a significant effect on tumor therapy, the most important issue is ensuring that CPT reaches target cells effectively. However, CPT's low bioavailability and its dispersibility problem within body fluids make it difficult for CPT to reach target cells. Such situations create a need for new and solution-oriented carrier and delivery systems[9].

The filamentous M13 bacteriophage stands out as a biocompatible nanocarrier platform due to its advantages, including non-infectivity of mammalian cells, a filamentous structure with a high surface area, and ease of production and purification. In particular, the ability of hydrophobic small molecules to form complexes with phage coat proteins through physical adsorption is considered a practical approach for transporting compounds with low water dispersibility into cells. This study aimed to use the M13 phage as a carrier system to facilitate the delivery of cryptotanshinone into cells without the need for any targeting ligand. In this research, the effect of cryptotanshinone on the biological behaviors of MCF-7 cells was evaluated *via FOXM1* gene expression; additionally, the comparative functional contribution of a carrier approach based on the delivery of CPT *via* M13 phage was investigated in comparison with free CPT application.

MATERIALS AND METHODS

Cell Culture

MCF-7 (HTB-22-ATCC, Manassas, VA, USA) cells were maintained in RPMI-1640 supplemented with 10% (v/v) heat-inactivated fetal bovine serum (FBS) and 2.5 mM L-glutamine, under standard culture conditions (37°C, 5% CO_2). Passaging was repeated every three days until a sufficient number of cells was reached for experiments. Cell counting was performed using the Cedex XS system (Roche Diagnostics, Mannheim, Germany).

Cells were washed with 2 mL sterile phosphate-buffered saline (dPBS) prewarmed to 37°C. After the remaining buffer was removed, 0.25 mL Trypsin-EDTA was added to the cells and incubated at 37°C for 5 minutes. The trypsinized cells were transferred into a 15 mL Falcon tube, and medium was added. The cell suspension was centrifuged at 130 × g for 5 minutes, and then the supernatant was removed. The resulting cell pellet was resuspended in 1 mL of supplemented medium. The cells were then left for incubation in a 5% CO_2 environment[10].

MCF-7 cells were verified to be mycoplasma-negative, and cells within the P5–20 passage range were used in experiments.

Reagents and Preparation of Cryptotanshinone Solutions

Before the experiment, cryptotanshinone was prepared as a 10 mM stock solution in dimethyl sulfoxide (Isolab GmbH, Eschau, Germany) under sterile conditions. In all applications used in experiments, the final DMSO concentration was kept constant among groups and adjusted not to exceed 0.1%.

MTT dye, a 5 mg/mL MTT stock solution in sterile phosphate buffer before use, was passed through a 0.22 µm filter to ensure sterility. CPT working solutions were prepared by serial dilution from the 10 mM DMSO stock, and the final DMSO concentration was equalized across all groups to ≤0.1%. The same ratio of DMSO was added to the negative control group[11].

MTT Cytotoxicity Analysis and IC_{50} Determination

In this study, the cytotoxicity of cryptotanshinone was evaluated using the MTT assay as previously described. To determine effective doses, CPT was tested at concentrations of 1, 10, 20, 40, and 80 µM[4]. Cell counting was performed using the Cedex XS cell analyzer (Roche Diagnostics, Mannheim, Germany). For the MTT analysis, cells from two 100% confluent flasks were seeded into three separate 96-well plates, with 200 µL of medium per well. After seeding, cells were incubated for 24 hours to allow attachment to the bottom of the wells.

MCF-7 cells were treated with medium containing the determined CPT concentrations (1, 10, 20, 40, and 80 µM) and incubated for 24 and 48 hours (for each concentration, n = 8 technical replicates), and experiments were conducted with at least three independent repeats. At the end of the incubation period, 20 µL MTT solution (5 mg/mL in PBS) was added to each well on top of the existing medium volume, and the plates were incubated at 37°C for 4 hours. With this process, the final volume in each well was standardized to 220 µL. After MTT incubation, the medium was removed and 100 µL DMSO was added to each well to dissolve the formed formazan crystals[12].

Absorbance values were measured at 570 nm using an ELISA microplate reader. IC_{50} values were calculated from dose-response curves generated using the percentages of cell viability obtained against different CPT concentrations. IC_{50} calculations were performed using GraphPad Prism software (GraphPad Software, San Diego, CA, USA) based on a 4-parameter logistic regression analysis using a log(dose)-response (variable slope) model[13].

Gene Expression Analysis (qRT-PCR)

Total RNA isolation was performed from the MCF-7 cell line. For this purpose, 1×10^6 cells suspended in 200 µL PBS were used for each of the control group and the groups treated with CPT at the determined doses (24 and 48 hours). Total RNA isolation was performed using the High Pure RNA Isolation Kit (Roche Diagnostics, Mannheim, Germany, Cat. No.: 1828665) according to the manufacturer's instructions[14].

cDNA synthesis was performed using the High-Capacity cDNA Reverse Transcription Kit (Thermo Fisher Scientific, Waltham, MA, USA, Cat. No.: 4368814) according to the kit protocol. The reaction mixture consisted of 10× RT Buffer, 25× dNTP Mix (100 mM), 10× RT Random Primers, MultiScribe™ Reverse Transcriptase, Nuclease-free H_2O, and total RNA. The prepared mixture was incubated in a thermal cycler sequentially at 25°C for 10 minutes, 37°C for 120 minutes, and 85°C for 5 minutes. As a result of this process, complementary DNA (cDNA) was obtained for use in further analyses[15].

As a housekeeping gene, *ACTB* (β-actin) (ACTB; ID: Hs99999903, Thermo Fisher Scientific, Waltham, MA, USA) and as target genes, *FOXM1* and *Cyclin B1* (*CCNB1*) expression levels were analyzed using the Real-Time RT-PCR method with the LightCycler 480 Probes Master kit (Roche Diagnostics, Mannheim, Germany). All procedures were carried out according to the protocol recommended by the manufacturer. Ct values were analyzed using the $2^{-\Delta\Delta Ct}$ method with the *ACTB* reference gene. Each sample was run in three technical replicates; no-template control (NTC) and no-RT controls were included in the experiments. RNA purity (A260/A280) was measured, and samples meeting appropriate quality criteria were used. Equivalent amounts of cDNA were used in each qPCR reaction. Stable expression of the *ACTB* gene under experimental conditions was confirmed. All gene expression analyses were performed on samples obtained from at least three independent experiments[16,17].

Detailed information regarding the reagents, instruments, and TaqMan assays used in the qRT-PCR experiments is provided in Supplementary Table 1.

Experimental Design Based on M13 Bacteriophage

To evaluate the carrier effect of M13 phage for CPT, the following experimental groups were created for cell viability (MTT) and *FOXM1* gene expression (qRT-PCR) analyses.

- Group 1 (control): cell + culture medium containing 0.1% (v/v) DMSO.
- Group 2 (M13 control): drug-free M13 phage (at the selected dose). Only the M13 phage suspension was added to the cells.
- Group 3 (free CPT): free CPT at the determined concentrations of $1\times IC_{50}$ and $0.5\times IC_{50}$. (The IC_{50} value was determined in preliminary experiments for the MCF-7 cell line, and at these doses, CPT was added directly to the culture medium.)

- Group 4 (CPT + M13 mixture): CPT and M13 phage applied simultaneously without loading. That is, free CPT (1×IC_{50} or 0.5×IC_{50}) and drug-free M13 phage were added to the cells at the same time.
- Group 5 (M13–CPT): cells treated with preformed M13–CPT complexes. The applied complex was adjusted to provide CPT-equivalent doses (1×IC_{50} or 0.5×IC_{50}) based on the measured loading efficiency.
- Group 6 (PEG/NaCl M13 control): drug-free M13 subjected to the same PEG/NaCl precipitation and washing steps used for Group 5.

Preparation of M13 phage and making it suitable for cell culture

In the study, filamentous M13 (M13 Sigma-Aldrich St. Louis, MO, USA - D4404) bacteriophage was used. For amplification of phages, the E. coli ER2738 strain was prepared as a starter culture in LB medium containing 20 µg/mL tetracycline and incubated overnight at 37°C with shaking at 200 rpm. The next day, the culture was diluted 1:100 with fresh medium, transferred to a larger volume medium, and infected with M13 phages[18].

The phage culture was incubated at 37°C with shaking at 250 rpm for 5 hours. After incubation, bacterial cells were removed by centrifugation, and the supernatant was transferred into a sterile tube. In phage-based experiments, cells were treated with relevant agents for 24 hours; MTT and qRT-PCR analyses were performed as specified in the relevant sections. During the experimental period, cells were incubated under standard culture conditions (37°C, 5% CO_2). Phage suspensions to be used in cell experiments were passed through 0.22 µm filtration and repeated PEG/NaCl precipitation/wash steps to reduce bacterial residues[19].

Determination of the bacteriophage titer

The titer of bacteriophages was determined by calculating the number of bacteriophages in each milliliter of sample, and the results were given as plaque-forming units (pfu/mL).

Dilutions were prepared from the bacteriophage stock in liquid culture with SM buffer from 10^{-1} to 10^{-8}. From each dilution, 300 µl phage and 1,000 µl from the overnight indicator bacteria liquid culture were taken, mixed with 4 mL top agar 0.4% at 45-48°C, immediately poured onto plates prepared beforehand, and incubated at 37°C for 1 night. After incubation, phage titers were determined by counting the phage plaques formed in the Petri dishes. The phage titer was determined as 1×10^{13} pfu/mL and this phage concentration was used in the studies[20].

Determination of the M13 phage dose applied to cells

The M13 phage dose to be used in cell experiments was determined within a biologically meaningful and non-cytotoxic range. For this purpose, reported doses indicating that filamentous phages do not show toxic effects on mammalian cells and are generally safely used in the range of 10^{7}–10^{10} pfu/mL were taken as a basis.

In this study, 5×10^{3} cells were seeded into each well of a 96-well plate, and the amount of M13 phage applied to the cells was adjusted to be a total of 1×10^{9} pfu per well. Under these conditions, the number of phages per cell is approximately:

$$\text{pfu/cell} = 1\times10^{9} \text{ pfu} / 5\times10^{3} \text{ cells} \approx 2\times10^{5} \text{ pfu/cell was calculated.}$$

The selected M13 phage dose (G2) was determined based on control group results that did not produce a significant effect on cell viability[21].

CPT loading procedure onto M13 phage

Cryptotanshinone (CPT) was loaded onto filamentous M13 phage by physical adsorption (including hydrophobic and π–π interactions). All loading and purification steps of CPT were performed in PBS (pH 7.4).

For use in the study, M13 phage stock was prepared at a concentration of 1×10^{13} pfu/mL. For the loading process, a phage suspension containing 1×10^{12} pfu in a total volume of 1 mL was prepared. For this purpose, 100 µL of M13 phage stock (1×10^{13} pfu/mL) was diluted with 900 µL PBS to obtain a total volume of 1 mL containing 1×10^{12} pfu phage particles[22].

From the 10 mM stock solution of cryptotanshinone prepared in DMSO, 1 µL CPT stock solution was added to 1 mL M13 phage suspension. Under these conditions, the final DMSO ratio was kept below 0.1%. Due to the light sensitivity of CPT, the M13–CPT mixture was incubated in light-proof (amber) tubes at room temperature (22-25°C) on an orbital shaker at 50 rpm for 12 hours (or overnight). After incubation, PEG/NaCl precipitation was applied to remove unbound free CPT. For this purpose, 0.25 mL (25% by volume) of a precipitation solution containing 20% (w/v) PEG-8000 and 2.5 M NaCl was added to 1 mL of the M13–CPT mixture. The mixture was mixed at 50 rpm and then incubated at 4°C for 1 hour. Then, samples were centrifuged at 10,000×g at 4°C for 10-20 minutes. After centrifugation, the supernatant was carefully removed, and a phage-containing pellet was obtained. The obtained pellet was resuspended in 100-200 µL PBS in a way that would preserve the structural integrity of the phages. At this stage, phage concentration before and after precipitation was verified by the plaque assay method (pfu/mL). PEG/NaCl precipitation was repeated twice to ensure the removal of free CPT. Thus, the M13–CPT complex in which cryptotanshinone was loaded onto the M13 phage, and free CPT was largely removed, was obtained. The M13–CPT complexes prepared using this method were stored at 4°C and under light-protected conditions before being used in cell experiments. CPT stocks were prepared in DMSO, and in all CPT-containing conditions, the final DMSO ratio was adjusted to ≤0.1 (v/v); the same DMSO ratio was added to control wells to equalize solvent effect[23].

Determination of cryptotanshinone loading efficiency

The loading efficiency of CPT onto M13 phage was calculated by quantitatively determining the amount of free CPT remaining in the supernatant after the PEG/NaCl precipitation process. For this purpose, after the loading procedure was completed and the M13–CPT complex was pelleted by centrifugation, the obtained supernatant was collected and analyzed.

The free CPT concentration in the supernatant was quantified by measuring at CPT's specific maximum absorbance wavelength (λ max ≈ 270-275 nm) using a UV–Vis spectrophotometer. Measurements were quantified with the help of a CPT standard curve prepared using a PBS/DMSO (0.1 v/v) mixture. The standard curve was prepared using the same solvent matrix (PBS + 0.1% DMSO) as the supernatant samples. The standard curve was generated using known CPT concentrations and linear regression analysis was applied ($R^2 > 0.99$).

Loading efficiency (%) was calculated using the following equation: Loading efficiency (%) = (Initial amount of CPT − Amount of free CPT in the supernatant) / Initial amount of CPT × 100.

Phage-containing samples were prepared at equivalent pfu/mL concentration, and CPT-containing samples were prepared at equivalent CPT concentration[24].

Statistical Analysis

Cell viability experiments were carried out to include technical replicates for each condition and experiments were repeated as at least three independent experiments (biological replicates). The mean of technical replicates was taken to obtain a single value for each independent experiment; statistical analyses were performed based on values obtained from independent experiments (n = number of independent experiments). Results were reported as mean ± standard deviation (mean ± SD).

Statistical analyses were performed using GraphPad Prism software (GraphPad Software, San Diego, CA, USA). Each time point (24 hours and 48 hours) was evaluated separately; intergroup comparisons were performed with one-way analysis of variance (one-way ANOVA). Dunnett's multiple comparisons test was used to compare multiple groups against the control group. In cases where the normality assumption was not met, appropriate non-parametric tests (Kruskal-Wallis and Dunn multiple comparisons test) were preferred. In all analyses, the significance level was accepted as $p < 0.05$.

IC_{50} values were calculated by fitting dose-response data to a four-parameter logistic model (variable slope, 4PL) by nonlinear regression and were reported together with 95% confidence intervals[25-27].

All experiments were performed using three independent biological replicates, each derived from separately cultured cell populations. Each qPCR reaction was carried out in technical triplicate to minimize analytical variability. Ct values were normalized to the reference gene *ACTB* and converted to ΔCt values. Statistical analyses were performed using ΔCt values rather than transformed fold-change data.

Characterization of M13–CPT nanocarrier system

Loading efficiency was quantified by measuring unbound cryptotanshinone (CPT) in the supernatant after PEG/NaCl precipitation using UV–Vis spectrophotometry (λ max ≈ 270-275 nm) against a matrix-matched calibration curve (PBS, 0.1% DMSO; $R^2 > 0.99$). Formulation stability was assessed by incubating M13–CPT complexes in PBS (pH 7.4, 37°C, 24 h), followed by quantification of released CPT in the supernatant. Reproducibility was evaluated across independent batches (n = 3), and loading efficiency was reported as mean ± SD[24].

Flow-Cytometric Analysis of Cellular Uptake

MCF-7 cells were seeded in 6-well plates at a density of 2×10^5 cells per well and allowed to attach overnight under standard culture conditions (37°C, 5% CO_2). Cells were then treated with free CPT or M13–CPT at equivalent CPT concentrations for 4 h, while untreated/vehicle-treated cells served as the control group. Following incubation, cells were washed three times with ice-cold PBS to reduce unbound extracellular material, detached using trypsin-EDTA, collected by centrifugation, and resuspended in PBS containing 1% FBS. Cell-associated CPT fluorescence was quantified by flow cytometry. Forward- and side-scatter gating was applied to exclude debris and cell aggregates, and at least 10,000 events were acquired per sample. Mean fluorescence intensity (MFI) was used as the primary quantitative index of relative cellular association/uptake. Data were obtained from three independent experiments and are presented as mean ± SD. Statistical significance was determined using one-way ANOVA followed by Tukey's multiple-comparisons test[21]. Samples were analyzed using a BD FACSCanto II flow cytometer, and data were processed using FlowJo software (version 10.6.2; BD Biosciences, Ashland, OR, USA).

Apoptosis analysis

Apoptosis in MCF-7 cells was evaluated by Annexin V-FITC/Propidium Iodide (PI) double staining followed by flow cytometry. Cells were seeded in 6-well plates at a density of 2×10^5 cells per well and allowed to reach approximately 70% confluence prior to treatment. Cells were then treated with the experimental groups (control, M13, CPT, CPT+M13, and M13–CPT) for 24 h. Following incubation, the cells were collected, washed twice with cold PBS, and resuspended in 100 µL of binding buffer (1×10^5 cells per sample). Cells were stained with Annexin V-FITC and PI using a commercial apoptosis detection kit (Annexin V-FITC Apoptosis Detection Kit, BD Biosciences, USA) and incubated for 15 min at room temperature (22-25°C) in the dark[26]. Samples were analyzed using a BD FACSCanto II flow cytometer (BD Biosciences, USA), and at least 10,000 events were acquired per sample. Data were analyzed using FlowJo software (version 10.6.2; BD Biosciences, Ashland, OR, USA), and cell populations were quantified based on quadrant gating as viable (Annexin V^-/PI^-), early apoptotic (Annexin V^+/PI^-), and late apoptotic (Annexin V^+/PI^+). All experiments were performed in three independent biological replicates. Data are presented as mean ± standard deviation (SD), and statistical analysis was performed using one-way ANOVA followed by Tukey's multiple comparisons test. A p-value <0.05 was considered statistically significant.

RESULTS

Effect of Cryptotanshinone on MCF-7 Cell Viability

The cytotoxic effect of the tested compound on the MCF-7 cell line was evaluated at different concentrations (1-80 µM) after 24 and 48 hours of incubation. Cell viability percentages were normalized to the control and analyzed using GraphPad Prism software (GraphPad Software, San Diego, CA, USA).

The dose-response relationship was modeled by nonlinear regression analysis separately for 24-hour and 48-hour data using a four-parameter logistic model (variable slope) (Figure 1C). At both time points, a marked decrease in cell viability was observed with increasing cryptotanshinone concentration, consistent with sigmoidal dose-response curves (Figure 1).

As a result of nonlinear regression analysis, the IC_{50} value was calculated as 19.82 µM (95% CI: 16.31-24.02 µM) for 24-hour treatment and 16.14 µM (95% CI: 13.17-19.69 µM) for 48-hour treatment. The obtained models showed high goodness-of-fit at both time points.

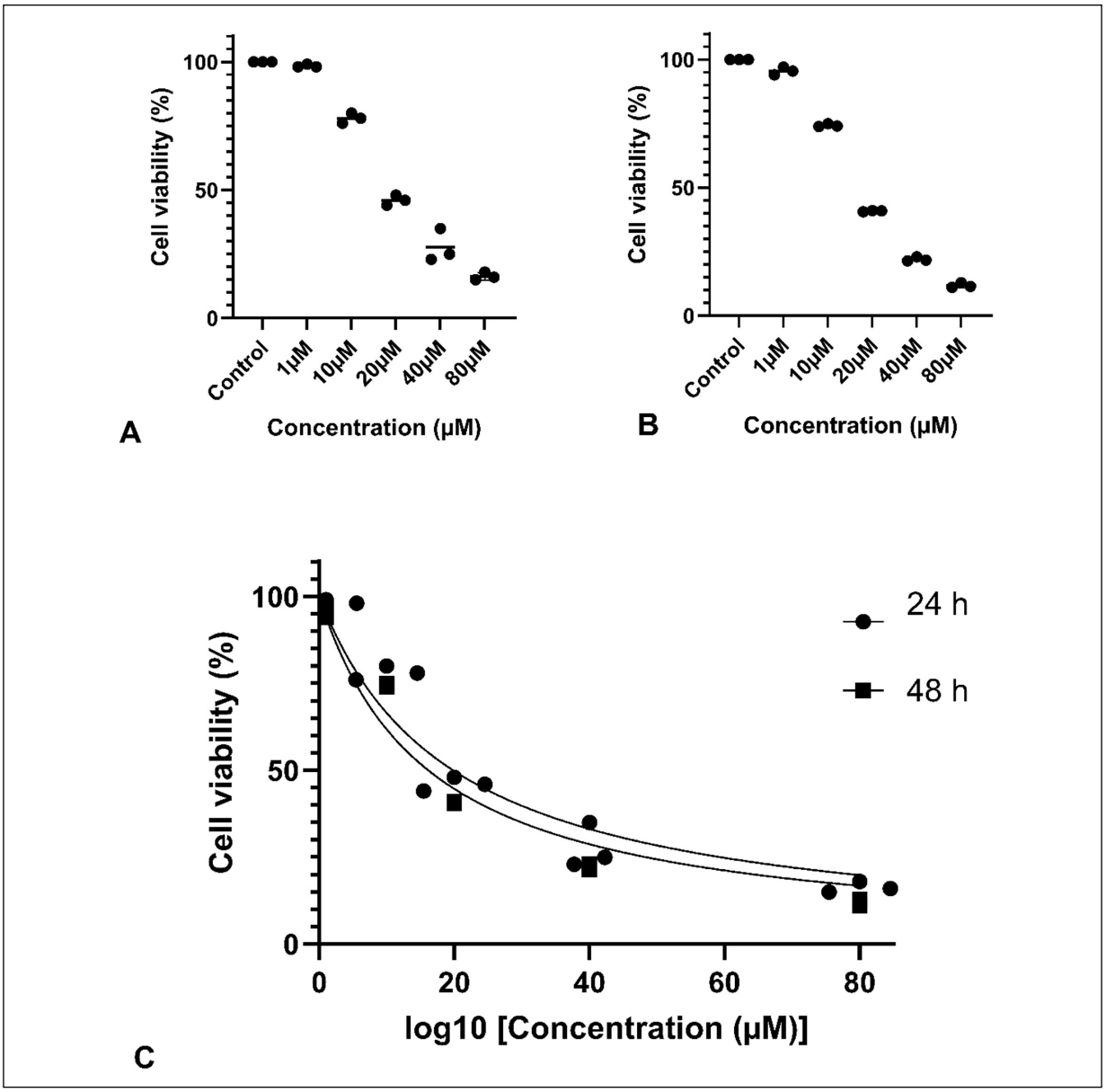

Figure 1. Effect of the compound on cell viability. **A**, Cell viability of MCF-7 cells after 24 h treatment. **B**, Cell viability after 48 h treatment. Data are shown as individual data points with mean ± SD. **C**, Dose–response curves and IC_{50} values at 24 h and 48 h obtained by nonlinear regression using a log(inhibitor) *vs.* response model.

Cell viability data are presented as mean ± standard deviation (mean ± SD). Differences among concentration groups were analyzed using one-way ANOVA and Dunnett multiple comparisons test, and a statistically significant decrease was detected at all concentrations of 10 μM and above compared to the control group ($p<0.0001$).

These findings reveal that cryptotanshinone exerts a dose- and time-dependent cytotoxic effect on MCF-7 cells and that cells become more sensitive to the compound with longer incubation time (Figure 1).

Evaluation of the Time-Dependent Cytotoxic Effect of Cryptotanshinone

The time-dependent cytotoxicity of cryptotanshinone on MCF-7 cells was evaluated by comparing cell viability at 24 and 48 hours of incubation. In applications performed over the same concentration ranges, it was determined that cell viability values at the end of 48-hour incubation were generally lower than those observed in 24-hour applications (Figure 1).

Especially at medium and high concentrations (≥20 µM), a more pronounced decrease in cell viability occurred with prolonged incubation. This indicates that the cytotoxic effect of cryptotanshinone increases not only with dose but also with exposure time.

These differences across time points indicate that the compound's effect on cells exhibits a cumulative character. The increased sensitivity of cells to cryptotanshinone with longer incubation time suggests that the compound's mechanism of action strengthens over time.

These findings demonstrate that cryptotanshinone exhibits a time-dependent cytotoxic effect in MCF-7 cells and support that the suppressive effect of the compound on cell proliferation increases with exposure duration.

Effect of CPT Application on FOXM1 Gene Expression

Two-way ANOVA analysis performed based on ΔCt values showed that treatment had a significant main effect (p<0.0001) and that there was a statistically significant interaction between treatment and time (p=0.0209). In contrast, the time factor alone was not found to be significant (p=0.0938). These findings reveal that the effect of cryptotanshinone on *FOXM1* gene expression varies over time.

Šidák's post-hoc analysis showed that CPT treatment significantly increased ΔCt values at 24 hours (p<0.05) and that this effect was more pronounced at 48 hours (p<0.01). The increase in ΔCt values indicates that *FOXM1* gene expression is suppressed (Figure 2, Table 1).

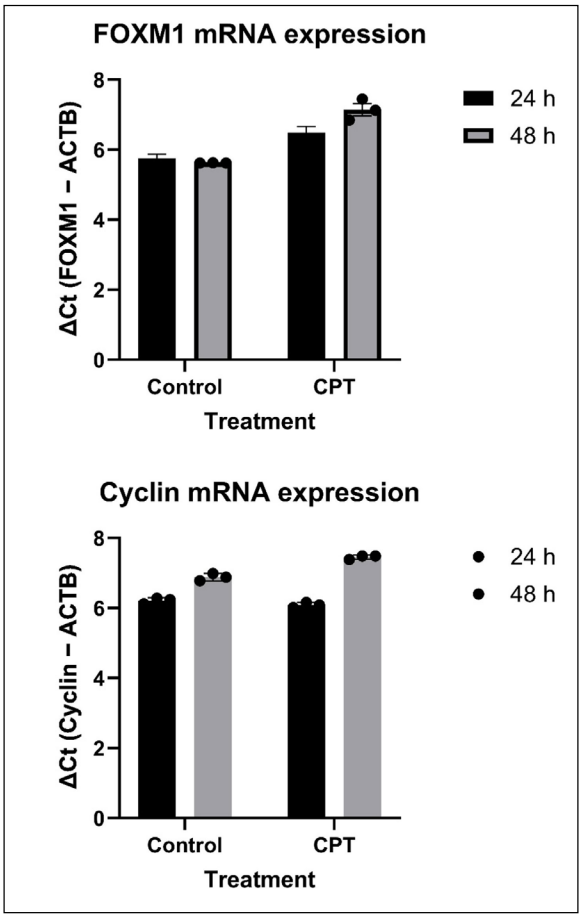

Figure 2. *FOXM1* mRNA expression. The effect of CPT treatment on *FOXM1* mRNA expression in MCF-7 cells after 24 and 48 hours is shown. *FOXM1* expression was normalized to the reference gene *ACTB* and expressed as ΔCt (*FOXM1* − *ACTB*). Data are presented as mean ± SD, with n = 3 independent biological replicates per group. Statistical analysis was performed using two-way ANOVA, and comparisons between groups at each time point were conducted using Sidak's post hoc test. p<0.05, *p<0.01 (comparison between Control and CPT at the corresponding time point).

Table 1. Effect of CPT treatment on *FOXM1* mRNA expression.

Time	Group	ΔCt (*FOXM1* − *ACTB*), Mean ± SD	n
24 h	Control	5.76±0.21	3
24 h	CPT	6.49±0.31*	3
48 h	Control	5.62±0.01	3
48 h	CPT	7.14±0.30**	3

Values are presented as mean ± SD (n=3). Statistical analysis was performed using two-way ANOVA followed by Sidak's multiple comparisons test. *p<0.05, **p<0.01 *vs.* control at the corresponding time point. Cryptotanshinone (CPT).

Effect of CPT Treatment on Cyclin B1 Gene Expression

Two-way ANOVA analysis performed based on ΔCt values showed that CPT treatment significantly affected *CCNB1* expression (p<0.001). Šidák's post-hoc comparisons demonstrated that CPT significantly increased ΔCt values at both time points compared with the corresponding control groups, indicating suppression of *CCNB1* expression.

At 24 h, CPT treatment significantly increased ΔCt values (p<0.05), while at 48 h the increase was more pronounced (p<0.01), suggesting a stronger downregulation of *CCNB1* expression with prolonged CPT exposure (Table 2).

Table 2. Effect of CPT treatment on *Cyclin B1* mRNA expression.

Time	Group	ΔCt (*Cyclin B1* − *ACTB*), Mean ± SD	n
24 h	Control	6.21±0.08	3
24 h	CPT	6.85±0.11*	3
48 h	Control	6.09±0.04	3
48 h	CPT	7.46±0.06**	3

Values are presented as mean ± SD (n=3). Statistical analysis was performed using two-way ANOVA followed by Sidak's multiple comparisons test. *p<0.05, **p<0.01 *vs.* control at the corresponding time point. Cryptotanshinone (CPT).

Cryptotanshinone Loading Efficiency onto M13 Phage

The loading efficiency of CPT onto filamentous M13 bacteriophage was determined by quantifying the amount of unbound CPT remaining in the supernatant following PEG/NaCl precipitation using UV–Vis spectrophotometric analysis. Based on the CPT standard calibration curve (R^2>0.99), the amount of CPT associated with the phage particles was calculated by subtracting the concentration of free CPT detected in the supernatant from the initial amount of CPT added to the loading system.

The loading efficiency was determined to be 55±3.2% (n=3 independent loading experiments), demonstrating reproducible association of CPT with the M13 phage particles. Considering that approximately 2.96 µg CPT was initially added to a system containing 1×10^{12} pfu of M13 phage, the amount of CPT associated with the phage particles corresponded to approximately 1.63 µg CPT per 10^{12} pfu M13.

These findings indicate that a substantial fraction of CPT molecules became associated with filamentous M13 phage particles during the loading process (Figure 3). Such association is consistent with the physical adsorption of hydrophobic small molecules onto phage coat proteins, as reported in previous studies[28].

Following PEG/NaCl precipitation and washing steps, the resulting M13–CPT complexes were resuspended in PBS and subsequently used in cell culture experiments at CPT-equivalent concentrations. The prepared complexes remained stable during short-term storage conditions, and no detectable release of CPT from the M13–CPT complexes was observed during the experimental time frame of the cellular assays, indicating that the phage-associated CPT remained stably bound under the applied experimental conditions.

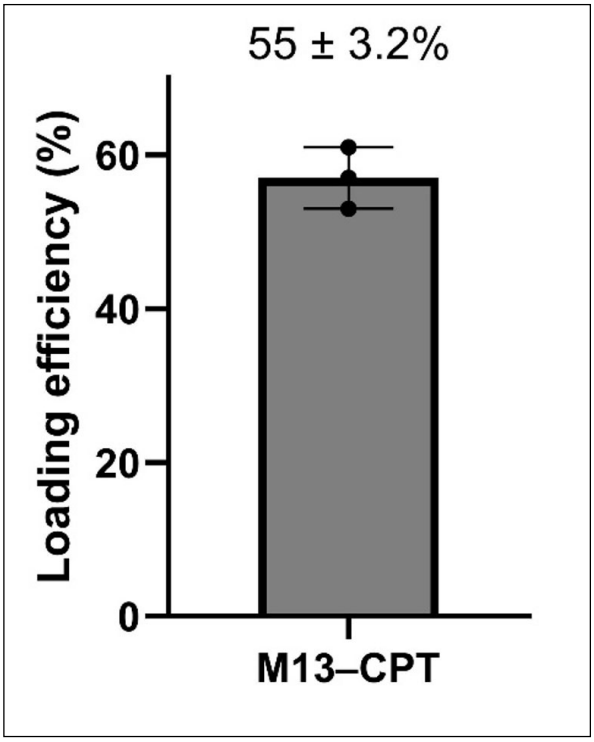

Figure 3. Loading efficiency of the M13–CPT nanocarrier system. Loading efficiency of cryptotanshinone (CPT) onto M13 bacteriophage. Data are presented as mean ± SD from three independent experiments (n=3), with individual data points shown.

Characterization of the M13–CPT nanocarrier system

The loading efficiency of CPT onto M13 bacteriophage was 55±3.2% (n=3), demonstrating consistent drug association across independent batches. Quantification was based on a linear calibration curve (R^2>0.99), confirming the reliability of the measurement approach. These results indicate that CPT can be reproducibly associated with M13 phage particles under the applied preparation conditions.

M13-Mediated Delivery Enhances Cellular Uptake of CPT

Flow cytometric analysis revealed a statistically significant difference among experimental groups [one-way ANOVA, F (2,6) = 1064, p<0.0001]. Quantitative analysis of mean fluorescence intensity (MFI) showed that control cells exhibited minimal background fluorescence (128.7±17.6), whereas treatment with free CPT resulted in a significant increase in cellular fluorescence (477.7±17.6, p<0.0001 *vs.* control), indicating baseline cellular association of the compound. Notably, cells treated with the M13–CPT formulation displayed a markedly higher MFI (936.3±17.6), which was significantly greater than both control and free CPT groups (p<0.0001) (Figure 4). These findings demonstrate that M13-mediated delivery significantly enhances the cellular association and uptake of CPT in MCF-7 cells.

Effect of M13 Phage-Mediated CPT Transport on Cell Viability

The effect of M13 phage-associated CPT (M13–CPT) on MCF-7 cell viability was evaluated using the MTT test. One-way ANOVA analysis showed that there were highly statistically significant differences among groups [F (4,10) = 768.7; p<0.0001].

Application of M13 phage alone did not produce a significant effect on cell viability compared to the control group (p>0.05). Free CPT application significantly reduced cell viability (Figure 5). Co-application of CPT and M13 without loading (CPT + M13) led to a limited but statistically significant additional decrease in cell viability compared to free CPT (Tukey, p<0.01).

In contrast, the group in which CPT was associated with M13 phage (M13–CPT) showed a marked and highly statistically significant decrease in cell viability compared to free CPT application (mean difference=24.0%; Tukey, p<0.0001). These findings indicate that the association of CPT with M13 phage can significantly enhance *in vitro* cytotoxic efficacy (Figure 5, Table 3).

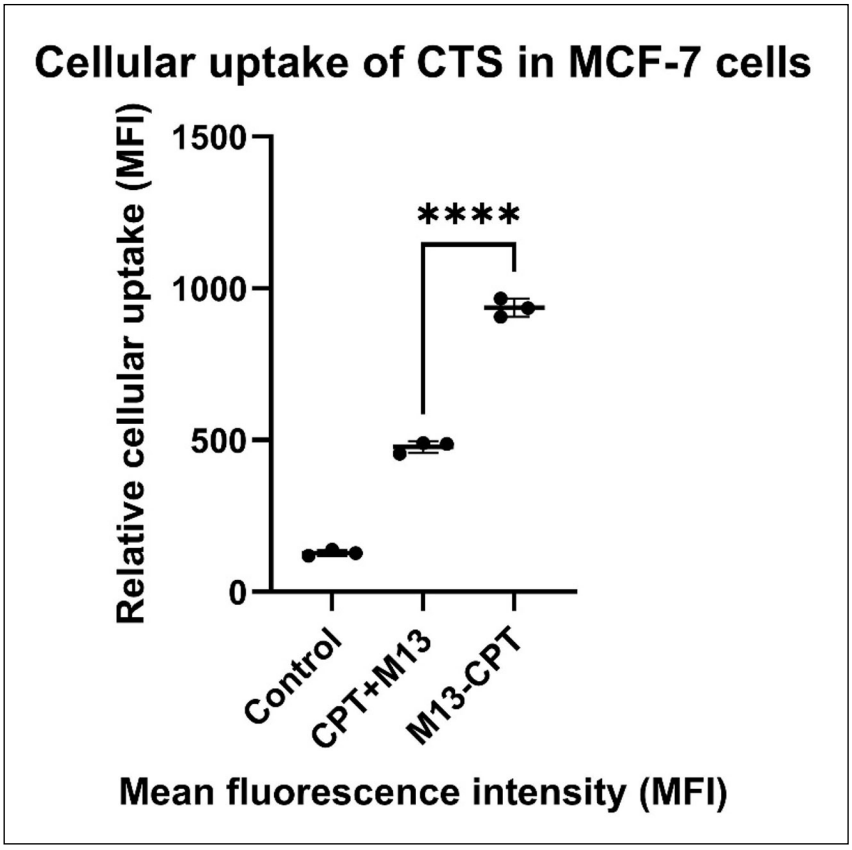

Figure 4. Flow-cytometric quantification of cellular uptake in MCF-7 cells. MCF-7 cells were treated with free cryptotanshinone (CPT) or M13–CPT at equivalent CPT concentrations for 4 h, and cellular uptake was quantified by flow cytometry. Uptake was expressed as mean fluorescence intensity (MFI). Data are presented as mean ± SD from three independent experiments. Statistical significance was determined by one-way ANOVA with Tukey's post hoc test (**p*<0.05, ***p*<0.01, ****p*<0.001).

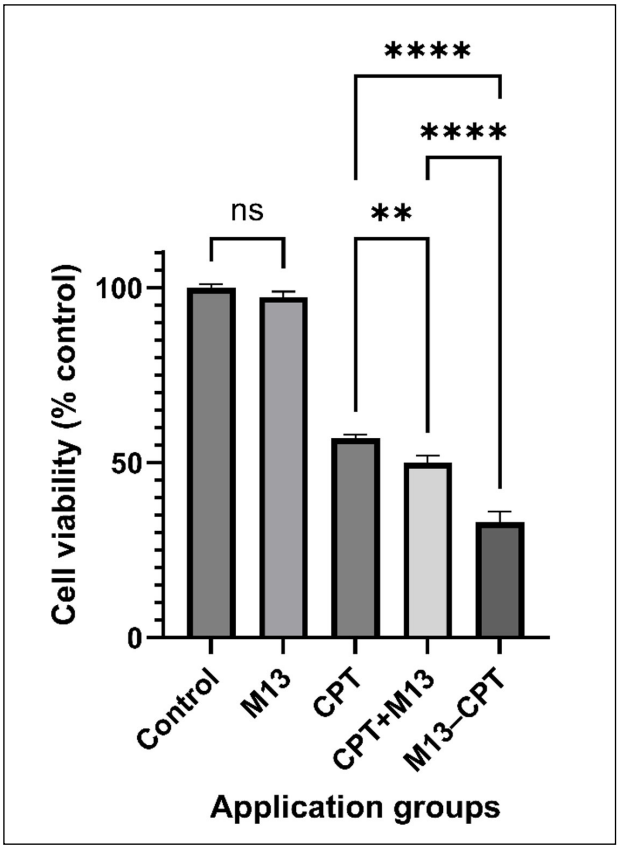

Figure 5. Effect of M13 phage-mediated CPT delivery on MCF-7 cell viability. Effect of M13-associated CPT (M13–CPT) on MCF-7 cell viability determined by MTT assay. Data are presented as mean ± SD (n=3). Statistical significance was determined by one-way ANOVA followed by Tukey's multiple comparisons test (**p*<0.05, ***p*<0.01, ****p*<0.001*;* ns, not significant).

Table 3. Effect of M13 phage-mediated CPT transport on MCF-7 cell viability.

Treatment group	Cell viability (% control, mean ± SD)
Control	100.0±1.0
M13	97.3±1.5
CPT	57.0±1.0
CPT + M13	50.0±2.0
M13–CPT	33.0±3.0

Values are given as mean ± SD (n=3 independent experiments). Cell viability was normalized to the control group. Statistical analysis was performed using one-way ANOVA and the Tukey multiple comparisons test. Cryptotanshinone (CPT).

M13-Mediated Delivery Enhances CPT-Induced Apoptosis

Annexin V-FITC/PI flow cytometry analysis revealed a statistically significant difference among experimental groups for both early and late apoptosis [one-way ANOVA, early apoptosis: $F(4,10)=151.3$, $p<0.0001$; late apoptosis: $F(4,10)=1346$, $p<0.0001$]. Early apoptosis levels were low in the control (2.37%) and M13 (2.88%) groups, with no significant difference between them ($p>0.05$). In contrast, CPT (13.33%), CPT+M13 (15.00%), and M13–CPT (20.93%) treatments significantly increased early apoptotic populations compared to control ($p<0.0001$). Notably, M13–CPT exhibited a significantly higher early apoptotic rate than free CPT ($p<0.01$). A similar trend was observed for late apoptosis. Control (2.13%) and M13 (2.67%) groups showed minimal late apoptotic fractions, whereas CPT (16.67%), CPT+M13 (21.03%), and M13–CPT (35.43%) groups demonstrated markedly elevated levels ($p<0.0001$). The highest late apoptosis was observed in the M13–CPT group, which was significantly higher than CPT alone ($p<0.0001$). These findings demonstrate that M13-mediated delivery significantly enhances CPT-induced apoptosis in MCF-7 cells (Figure 6).

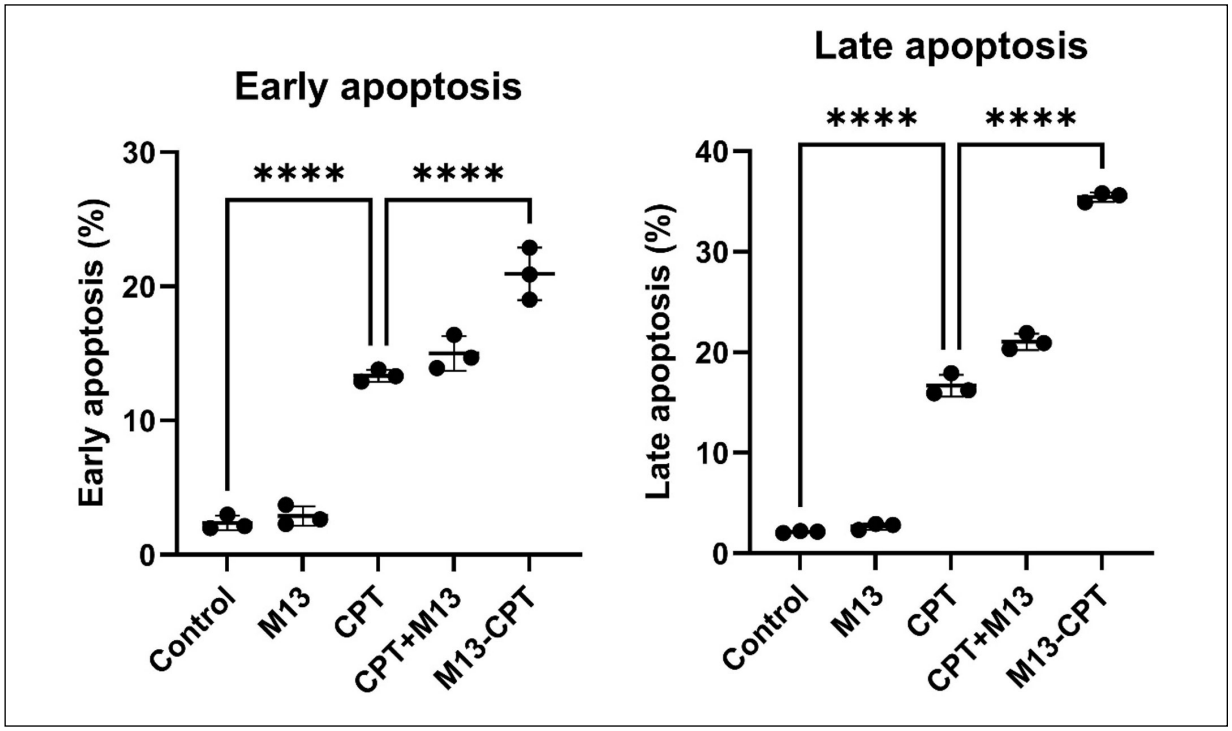

Figure 6. M13-mediated delivery enhances CPT-induced apoptosis. **A**, Early and (**B**) late apoptosis in MCF-7 cells were assessed by Annexin V-FITC/PI flow cytometry after 24 h treatment. CPT significantly increased apoptosis compared to control, while M13–CPT further enhanced apoptosis relative to free CPT ($p<0.0001$). Data are presented as mean ± SD (n=3); one-way ANOVA with Tukey's test.

DISCUSSION

The results obtained from this study showed that cryptotanshinone has a marked antiproliferative and proapoptotic effect on MCF-7 breast cancer cells. In particular, it was observed that using M13 phage as a drug delivery system significantly increased the cell-killing effect of CPT, with a statistically significant difference. The results of the MTT experiment, conducted to determine cytotoxicity, showed that CPT significantly reduced the viability of MCF-7 cells, depending on dose and application duration. The IC_{50} value, approximately 20 µM at 24 hours, decreased to approximately 16 µM at 48 hours, indicating that cells became more sensitive to CPT with prolonged exposure. Similarly, previous studies show that the cytotoxic efficacy of CPT in a breast cancer cell line increases as the application duration is prolonged. In this context, our results are consistent with the literature[4,29]. According to the literature, the underlying mechanisms of CPT's suppressive effect on cell proliferation include arresting the cell cycle at the G2/M phase and inducing apoptosis. For example, Shi et al[4] reported that CPT arrested the cell cycle at the G2/M phase in MCF-7 cells and reduced the levels of key cell cycle proteins such as Cyclin A, B, and D[30]. Our findings are in parallel with this study. In other words, our results support the potential of CPT to induce dose-dependent growth suppression in breast cancer cells.

One of the important findings of our study is that CPT suppresses *FOXM1* gene expression. The *FOXM1* gene stands out as a transcription factor that plays a critical role, especially in mitotic progression and the regulation of the G2/M transition of the cell cycle. Research[30] conducted in recent years shows that in many cancer types, overexpression of the *FOXM1* gene causes rapid tumor growth, metastatic potential, and poor prognosis. Therefore, changes in *FOXM1* expression levels are considered an important indicator in the evaluation of parameters such as tumor aggressiveness and treatment response. In our experiments, CPT treatment significantly reduced *FOXM1* mRNA level compared to the control group after 24 hours; at 48 hours, this suppression became even more pronounced (increase in ΔCt, $p<0.01$). This decrease in *FOXM1* expression can be considered as a molecular reflection of CPT's antiproliferative effect. Indeed, studies[30,31] in the literature report that tanshinone-derived compounds can exhibit an antitumor effect by down-regulating *FOXM1* in cancer cells. For example, in one study[31], tanshinone IIA was reported to suppress cell proliferation by reducing *FOXM1* expression in gastric cancer cells. In parallel with these findings, our study suggests that CPT may interfere with cell-cycle–related regulatory pathways through a mechanism targeting *FOXM1* in breast cancer cells. The underlying mechanism of this situation can be explained as follows: suppression of *FOXM1* may render cells unable to express genes required for mitosis, thereby affecting genes involved in mitotic progression and the G2/M transition, and consequently making cancer cells more prone to programmed cell death[32]. Therefore, our results show that CPT can inhibit tumor cell proliferation by altering *FOXM1* expression. Given the known oncogenic role of the *FOXM1* gene, down-regulating it may be an important strategic target in cancer therapy. In addition to *FOXM1* downregulation, CPT treatment also reduced the expression of the downstream mitotic regulator *Cyclin B1* (*CCNB1*). Since *Cyclin B1* is a well-established transcriptional target of *FOXM1* involved in the regulation of the G2/M transition, this finding suggests that CPT may interfere with *FOXM1*-associated mitotic regulatory pathways. The coordinated reduction of *FOXM1* and *Cyclin B1* expression, therefore, supports the possibility that CPT modulates proliferation-related signaling networks linked to *FOXM1* activity in breast cancer cells. Importantly, this molecular effect was functionally supported by apoptosis analysis, which demonstrated a significant increase in both early and late apoptotic cell populations following CPT treatment, with a further pronounced enhancement observed in the M13–CPT group. These findings provide functional evidence that *FOXM1* downregulation may be associated with apoptosis-mediated mechanisms contributing to the observed antiproliferative effect.

Another original and important outcome of our study is the results obtained with M13 phage as a CPT carrier. While M13 phage alone did not affect cell viability (the phage control group remained at the control level with ~97% viability), delivering CPT loaded onto M13 phage at the same concentration reduced cell viability markedly more compared to free CPT. In particular, it was observed that application of the M13–CPT complex at equivalent doses reduced the viability rate of free CPT from ~57% down to ~33% (an additional decrease of approximately 24%). This pronounced difference showed that phage-mediated delivery of CPT markedly enhanced its functional cytotoxicity *in vitro* and the drug substance's efficacy. The mechanisms underlying the higher cytotoxicity of phage-delivered CPT can be explained as follows: (i) M13 phage, with its filamentous structure and high surface area, can act as a nano-carrier and carry many CPT molecules on its surface; (ii) hydrophobic CPT molecules can adsorb to phage surface proteins, potentially improving their dispersibility in aqueous environments; (iii) by interacting with the cell surface, phage particles may facilitate the interaction of CPT to cancer cells; however, this possibility was not directly examined in the present study[33]. In the literature, some studies[34] have shown that filamentous phages such

as M13 can deliver therapeutic payloads they carry into cells while exhibiting a biocompatible profile. M13 phage, which infects only *E. coli* bacteria and cannot replicate in mammalian cells, is considered safe for humans[34]. With its safety profile for humans, M13 phage has been used in various fields such as drug delivery, bioimaging, and targeted therapy applications, and has been addressed as an innovative bionanomaterial. According to our findings, the phage itself could serve as a cargo carrier without causing significant cell toxicity (viability at the control level). Consistent with this observation, the significantly higher cellular uptake detected in the M13–CPT group further supports the role of M13 phage as an effective delivery platform facilitating intracellular availability of CPT.

The present results indicate that M13-mediated delivery significantly enhanced the functional cytotoxic efficacy of CPT in MCF-7 cells. Importantly, this interpretation is supported by our flow cytometric uptake analysis, which demonstrated a significant increase in mean fluorescence intensity in the M13–CPT group compared with free CPT, indicating enhanced cellular association and uptake of the phage-mediated formulation. Therefore, the observed enhancement should be interpreted cautiously and cannot yet be attributed to a specific uptake mechanism. Previous studies[35,36] have demonstrated that filamentous bacteriophages such as M13 can be internalized by mammalian cells and may serve as biocompatible nanocarriers capable of facilitating intracellular transport of therapeutic molecules. In this context, the increased cytotoxic activity observed in the M13–CPT group may reflect improved cellular accessibility or localized delivery of CPT; however, direct uptake imaging and intracellular drug quantification will be necessary to clarify the exact mechanism in future studies. Rather, the observed enhancement in biological activity may reflect improved dispersibility of CPT in the cell culture environment and/or more effective localized presentation of the compound to cancer cells. This enhanced uptake provides a mechanistic basis for the increased cytotoxic and pro-apoptotic effects observed in the M13–CPT group, linking improved intracellular delivery to the observed biological outcomes. The observed loading efficiency (55±3.2%) and its reproducibility across independent batches further support the reliability of the M13–CPT nanocarrier system under the applied experimental conditions.

In clinical trials[37], the problems of low water dispersibility and bioavailability of cryptotanshinone are the main obstacles preventing widespread use of this molecule. Application of CPT *via* non-toxic nanocarrier systems can contribute to delivering the drug to target tissues at an effective dose and reducing side effects. For example, in a study conducted by Zhao et al[38], it was reported that prepared CPT nanocrystals provided a ~64-fold increase in dispersibility and a ~2.9-fold improvement in oral bioavailability compared to the raw drug. The M13 phage used in our study may have improved the dispersibility of CPT in the cell culture environment, thereby facilitating its interaction with cells; however, no direct dispersibility or dissolution measurements were performed in the present study. The slight additional decrease in cell viability in the group where free CPT and M13 phage were co-applied (from 57% to 50%) indicates that the phage may have facilitated the distribution of CPT into the medium and its transport to the cell surface. Although the CPT + M13 combination produced a modest additional reduction in cell viability compared with CPT alone, a formal pharmacological interaction analysis was not performed in the present study. Approaches such as Bliss independence, Loewe additivity, or Chou–Talalay combination index analysis could provide a more rigorous quantitative assessment of potential synergistic or additive interactions between CPT and M13. However, such analyses require systematic multi-dose combination experiments, which were beyond the scope of the current study. Future studies, including comprehensive dose-combination designs, may allow a more detailed characterization of the interaction between CPT and phage-based delivery systems. Importantly, this effect should be interpreted as improved dispersibility rather than true solubility, as no direct solubility measurements were performed in the present study.

However, the most pronounced effect was obtained by pre-loading CPT onto the phage and removing the remaining free drug[23]. It can be hypothesized that the M13–CPT complex may increase cytotoxicity by improving the dispersibility of CPT in the culture environment and enhancing its accessibility to cancer cells; however, the precise cellular uptake mechanism was not directly investigated in the present study. In the literature, studies[33] report the use of genetically modified phages as targeted drug carriers, thereby significantly improving the uptake of chemotherapeutic drugs into cells and tumor accumulation. One study[39] showed that doxorubicin coated with folate-liganded M13 phage is taken up by folate receptor-positive cancer cells at a much higher rate than the free drug, and its cytotoxic efficacy is markedly increased. Similarly, although we did not add a specific targeting ligand, we observed that phage-mediated CPT transport increased drug efficacy *in vitro*. As a result, our findings support the view that phage-based carrier systems can provide a practical and effective solution, facilitating the passage of hydrophobic anticancer agents into cancer cells. In the present study, the cytotoxic activity of the M13–CPT complex was evaluated at the IC_{50}-equivalent concentration of CPT in order to directly compare the enhancement of cytotoxic efficacy relative to free CPT. While this strategy enables comparison at a biologically relevant dose, the inclusion of a full dose–response

analysis for M13–CPT would allow a more quantitative assessment of the magnitude of enhancement provided by phage-mediated delivery. Therefore, future studies including broader dose–response evaluations will be necessary to further characterize the pharmacological behavior of the M13-based delivery system.

In summary, it was understood that cryptotanshinone suppresses the growth of cancer cells in a hormone receptor-positive breast cancer cell line and may interfere with mitotic progression and proliferation-related pathways and the suppression of proliferation-related genes such as *FOXM1*. In particular, delivery of CPT with M13 bacteriophage significantly strengthened the effect of the drug on cells. With this innovative approach, association with M13 phage may improve the dispersibility of CPT in the experimental system and may facilitate its interaction with cancer cells. Our findings reveal that phage-based nano-carriers are promising in the field of cancer therapy, and in future studies, the efficacy and safety of this system should be investigated in *in vivo* models; additionally, the potential of targeted drug delivery should be improved by increasing specificity with strategies such as adding tumor-cell-targeting peptides to the phage surface. Thus, it may contribute to the development of more effective and specific treatment options in breast cancer.

Limitations

This study has several limitations that should be acknowledged. First, the biological evaluation was performed using only a single luminal breast cancer cell line (MCF-7). Breast cancer is a heterogeneous disease comprising multiple molecular subtypes, including luminal, HER2-positive, and triple-negative forms, each characterized by distinct biological behaviors and therapeutic responses. Therefore, although the present results demonstrate the antiproliferative activity of CPT and the enhanced functional efficacy of M13-mediated delivery in MCF-7 cells, the generalizability of these findings to other breast cancer subtypes cannot yet be established. Future studies should validate the observed effect in additional breast cancer models, including HER2-positive and triple-negative cell lines, and should also evaluate non-tumorigenic breast epithelial cells to assess cancer selectivity.

Although the results demonstrate enhanced CPT efficacy *via* M13-mediated delivery in MCF-7 cells, the use of a single cell line represents a limitation. Validation in additional breast cancer models with different molecular subtypes would further strengthen the generalizability of these findings. Future studies involving multiple cancer models and protein-level validation are warranted to further confirm the translational relevance of these findings.

CONCLUSIONS

In conclusion, cryptotanshinone produced a pronounced dose- and time-dependent reduction in MCF-7 breast cancer cell viability and significantly suppressed *FOXM1* expression, indicating a mechanistically coherent antiproliferative response in this hormone receptor–positive *in vitro* model. The observed temporal strengthening of *FOXM1* downregulation further supports that CPT-mediated growth inhibition is accompanied by transcriptional modulation of a key mitotic and cell cycle-associated regulator.

Importantly, CPT delivery *via* filamentous M13 bacteriophage (M13–CPT) potentiated cytotoxicity compared with free CPT and non-loaded co-administration, while the phage vehicle alone remained biologically inert under the experimental conditions. Collectively, these findings identify M13 as a biocompatible nano-carrier capable of enhancing the functional efficacy of poorly soluble anticancer small molecules without the need for additional targeting ligands, and justify further evaluation in advanced mechanistic and preclinical settings.

Funding:
No funding is declared for this article.

Authors' Contributions:
Mustafa Ustundag contributed to the study concept and design and performed all bacteriophage (M13) preparation, handling, and phage-associated cryptotanshinone (M13–CPT) experiments. He also contributed to data analysis and interpretation and drafted the original manuscript. Berrin Ustundag conducted the non-phage experimental procedures, including the cell culture experiments with free cryptotanshinone (CPT) and CPT+M13 co-administration, performed the MTT cell viability assays and qRT-PCR analyses, interpreted the results, critically revised the manuscript for important intellectual content, and approved the final version to be published. Both authors read and approved the final manuscript.

ORCID ID:
Mustafa Ustundag: 0000-0002-2990-4981
Berrin Ustundag: 0000-0001-5211-7874

Conflict of Interest:
The authors declare that they have no conflict of interest to disclose.

Data Availability:
All data generated or analyzed during this study are included in this published article.

Ethics Approval and Informed Consent:
This study was conducted using the established human breast cancer cell line MCF-7 and did not involve human participants, patient-derived materials, or experimental animals. Therefore, according to institutional and international research ethics guidelines, ethical committee approval and informed consent were not required.

REFERENCES

1. American Cancer Society. Cancer faCPT and figures 2025. Atlanta: American Cancer Society; 2025.
2. Giaquinto AN, Freedman RA, Newman LA. Lobular breast cancer statistics, 2025. CA Cancer J Clin 2025.
3. Telang N. The divergent effect of ovarian steroid hormones in the MCF-7 model for luminal A breast cancer: mechanistic leads for therapy. Int J Mol Sci 2022; 23: 4800.
4. Shi D, Li H, Zhang Z, He Y, Chen M, Sun L, Zhao P. Cryptotanshinone inhibits proliferation and induces apoptosis of breast cancer MCF-7 cells via GPER mediated PI3K/AKT signaling pathway. PLoS One 2022; 17: e0262389.
5. Rajabi S, Shakib H, Safari-Alighiarloo N, Maresca M, Hamzeloo-Moghadam M. Targeting autophagy for breast cancer prevention and therapy: from classical methods to phytochemical agents. Iran J Basic Med Sci 2024; 27: 1475-1491.
6. Zhao H, Cheng X, Yan L, Mi F, Wang W, Hu Y, Liu X, Fan Y, Min Q, Wang Y, Zhang W, Wu Q, Zhan Q. APC/C regulated CPT1C promotes tumor progression by upregulating the energy supply and accelerating the G1/S transition. Cell Commun Signal 2024; 22: 283.
7. Elbashir MK, Mohammed M, Mwambi H, Omolo B. Identification of hub genes associated with breast cancer using integrated bioinformatics analysis. Appl Sci 2023; 13: 2403.
8. Hasan MAM, Maniruzzaman M, Shin J. Differentially expressed discriminative genes and significant meta-hub genes in cancer diagnosis. Sci Rep 2023; 13: 1-15.
9. Perez-Ortega HU, Cordova-Espiritu RR, Cano-Serrano S, Garcia-Gonzalez E, Bravo-Sanchez MG, Orozco-Mosqueda M del C, Jimenez-Islas H, Luna-Barcenas G, Villasenor-Ortega F. Camptothecin in cancer therapy: current challenges and emerging strategies with nanoemulsions. Pharmaceutics 2025; 17: 1414.
10. Yilmaz S, Sarikaya MD, Bagci BS, Besparmak EA, Yasar E, Onal O, Canoz O. Determination of cancer stem cell proliferation in lung cancer patients: a pilot study. Bozok Tip Derg 2024. Available from: https://dergipark.org.tr/en/pub/bozoktip/issue/87196/1550260. (Accessed on: Jan 14, 2026).
11. Malakpour-Permlid A, Rodriguez MM, Zor K, Boisen A, Oredsson S. Advancing humanized 3D tumor modeling using an open access xeno-free medium. Front Toxicol 2025; 7: 1529360.
12. Tastan P, Armagan G, Dagci T, Kivcak B. Psephellus pyrrhoblepharus ekstrelerinin sitotoksik aktivitesi. Kahramanmaras Sutcu Imam Univ Tip Fak Derg 2021; 16: 231-238.
13. D'Ascola A, Irrera N, Ettari R, Bitto A, Pallio G, Mannino F, Atteritano M, Campo GM, Minutoli L, Arcoraci V, Squadrito V, Picciolo G, Squadrito F, Altavilla D. Exploiting curcumin synergy with natural produCPT using quantitative analysis of dose effect relationships in an experimental in vitro model of osteoarthritis. Front Pharmacol 2019; 10: 1347.
14. Xiong H, Nie X, Cao W, Zhu J, Chen J, Liu R, Li Y. Investigation of mitochondria dependent apoptosis pathway and lipid peroxidation level induced by biosynthesized silver nanoparticles: caspase-3 activation, BAK1/BCLx regulation and malondialdehyde production. Cancer Nanotechnol 2024; 15: 20.
15. Ocalewicz K, Kucinski M, Jasielczuk I, Gurgul A, Kucharski M, Dobosz S. Transcript level of telomerase reverse transcriptase (TERT) gene in the rainbow trout (Oncorhynchus mykiss) eggs with different developmental competence for gynogenesis. J Appl Genet 2024; 65: 897-905.
16. Leal MF, Astur DC, Debieux P, Arliani GG, Franciozi CE, Loyola LC, Andreoli CV, Smith MAC, Pochini AC, Ejnisman B, Cohen M. Identification of suitable reference genes for investigating gene expression in anterior cruciate ligament injury by using reverse transcription quantitative PCR. PLoS One 2015; 10: e0133323.
17. Applied Biosystems. TaqMan gene expression assays: genome wide collection of quantitative standardized assays. Available from: https://dbgap.ncbi.nlm.nih.gov/projeCPT/genome/probe/doc/ProjTaqMan.shtml (accessed Jan 14, 2026).
18. Blazic M, Gautier C, Norberg T, Widersten M. High throughput selection of new enzymes: phage display mediated isolation of alkyl halide hydrolases from a library of active site mutated epoxide hydrolases. Faraday Discuss 2024; 252: 115-132.
19. Huang K, Nitin N. Edible bacteriophage based antimicrobial coating on fish feed for enhanced treatment of bacterial infections in aquaculture industry. Aquaculture 2019; 502: 18-25.
20. Sada TS, Tessema TS. Isolation and characterization of lytic bacteriophages from various sources in Addis Ababa against antimicrobial resistant diarrheagenic Escherichia coli strains and evaluation of their therapeutic potential. BMC Infect Dis 2024; 24: 246.

21. Sittiju P, Wudtiwai B, Chongchai A, Hajitou A, Kongtawelert P, Pothacharoen P, Suwan K. Bacteriophage based particles carrying the TNF related apoptosis inducing ligand gene for targeted delivery in hepatocellular carcinoma. Nanoscale 2024; 16: 6603-6617.
22. Szymczak M, Pankowski JA, Kwiatek A, Grygorcewicz B, Karczewska-Golec J, Sadowska K, Golec P. An effective antibiofilm strategy based on bacteriophages armed with silver nanoparticles. Sci Rep 2024; 14: 59866.
23. Tai C, Liu C, Pan YC, Wong SH, Tai CJ, Richardson CD, Lin L. Chemovirotherapeutic treatment using camptothecin enhances oncolytic measles virus mediated killing of breast cancer cells. Sci Rep 2019; 9: 6767.
24. Needham PG, Page RC, Yehl K. Phage layer interferometry: a companion diagnostic for phage therapy and a bacterial testing platform. Sci Rep 2024; 14: 55776.
25. Tong W, Xiong H, Fang H, Wu Y, Li H, Huang X, Leng Y, Xiong Y. Bifunctional M13 phage as enzyme container for the reinforced colorimetric photothermal dual modal sensing of ochratoxin A. Toxins 2022; 15: 5.
26. Asici GSE, Kiral F, Bayar I, Bildik A, Ulutas PA. Cytotoxic and Apoptotic Effects of Curcumin on D-17 Canine Osteosarcoma Cell Line. Kafkas Univ Vet Fak Derg 2021; 27: 465-473.
27. Rodrigues ET, Pereira E, Oliveira PJ, Pardal MA. The H9c2(2-1) cell based sulforhodamine B assay is a non animal alternative to evaluate municipal wastewater quality over time. Environ Monit Assess 2023; 195: 1257.
28. Lim C, Ko J, Jeon D, Song Y, Park J, Ryu J, Lee DW. Probing molecular mechanisms of M13 bacteriophage adhesion. Communications Chemistry. 2019;2:96. doi:10.1038/s42004-019-0198-0.
29. Dalil D, Iranzadeh S, Kohansal S. Anticancer potential of cryptotanshinone on breast cancer treatment: a narrative review. Front Pharmacol 2022; 13: 979634.
30. Wei P, Zhang N, Wang Y, Li D, Wang L, Sun X, Shen C, Yang Y, Zhou X, Du X. FOXM1 promotes lung adenocarcinoma invasion and metastasis by upregulating SNAIL. Int J Biol Sci 2015; 11: 186-198.
31. Alam SSM, Samanta A, Uddin F, Ali S, Hoque M. Tanshinone IIA targeting cell signaling pathways: a plausible paradigm for cancer therapy. Pharmacol Rep 2023; 75: 907-922.
32. Wonsey DR, Follettie MT. Loss of the Forkhead transcription factor FOXM1 causes centrosome amplification and mitotic catastrophe. Cancer Res 2005; 65: 5181-5189.
33. Karimi M, Mirshekari H, Basri SMM, Bahrami S, Moghoofei M, Hamblin MR. Bacteriophages and phage inspired nanocarriers for targeted delivery of therapeutic cargos. Adv Drug Deliv Rev 2016; 106: 45-62.
34. Wang H, Yang Y, Xu Y, Chen Y, Zhang W, Liu T, Chen G, Wang K. Phage based delivery systems: engineering, applications, and challenges in nanomedicines. J Nanobiotechnol 2024; 22: 402.
35. Kim A, Shin TH, Shin SM, Pham CD, Choi DK, Kwon MH, Kim YS. Cellular internalization mechanism and intracellular trafficking of filamentous M13 phages displaying a cell penetrating transbody and TAT peptide. PLoS One 2012; 7: e51813.
36. Gorski A, Miedzybrodzki R, Wegrzyn G, Jonczyk-Matysiak E, Borysowski J, Weber-Dabrowska B. Phage therapy: current status and perspectives. Med Res Rev 2020; 40: 459-463.
37. Chen ZM, Hu J, Xu YM, He W, Meng L, Huang T, Ying SC, Jiang Z, Xu AM. Cryptotanshinone inhibits cytotoxin associated gene A associated development of gastric cancer and mucosal erosions. World J Gastrointest Oncol 2021; 13: 693-705.
38. Zhao W, Ruan B, Sun X, Yu Z. Preparation and optimization of surface stabilized cryptotanshinone nanocrystals with enhanced bioavailability. Front Pharmacol 2023; 14: 1122071.
39. Unida V, Vindigni G, Raniolo S, Stolfi C, Desideri A, Biocca S. Folate functionalization enhances cytotoxicity of multivalent DNA nanocages on triple negative breast cancer cells. Pharmaceutics 2022; 14: 2610.